Inverse parametric optimization method for the characterization of the acoustic field radiated by a rail with a microphone array

Baldrik Faure, Marie-Agnès Pallas, Christine Serviere

ACOUSTICS 2012

Inverse parametric optimization method for the characterization of the acoustic field radiated by a rail with a microphone array - Experimental validation with a modal shaker

B. Faure[a], O. Chiello[b], M.-A. Pallas[b] and C. Servière[c]

[a]SNCF, Direction de l'Innovation et de la Recherche, 40, avenue des Terroirs de France, 75611 Paris Cedex 12, France
[b]IFSTTAR, 25 avenue F. Mitterrand, case 24, 69675 Bron Cedex, France
[c]Grenoble Images Parole Signal Automatique, Gipsa-lab 961 rue de la Houille Blanche BP 46 F - 38402 Grenoble Cedex
baldrik.faure@sncf.fr

For speeds up to 300 km/h, rolling noise is the main railway noise source. It arises from the acoustic radiation of various elements such as wheels, rails or sleepers. The rail, which mainly contributes to rolling noise at mid-frequencies and dominates from approximately 500 Hz to 1000 Hz, is an extended coherent source for which classical array processing methods are inappropriate to noise source identification. The properties of the acoustic field radiated by the rail are heterogeneous with regard to space and frequency, and depend on the vibration waves that propagate along the rail through the structural wavenumbers. In this paper, an inverse parametric optimization method is proposed to characterize the acoustic field radiated by a rail from microphone array measurements. The unknown parameters of a vibro-acoustical model (amplitudes and complex wavenumbers) are estimated through the minimization of a least squares criterion applied to the measured and modelled spectral matrices of the array. First, simulations are performed in order to appraise the performance of the method, in the case of vertical point excitations on the rail. This simple case is then validated experimentally for a single vertical point excitation using a modal shaker and a horizontal linear array.

1 Introduction

In the existing context of railway transports development, the reduction of noise annoyance is a main issue that concerns many different actors, from the infrastructure owners to the railway operators, not forgetting the material manufacturers. In order to tackle noise at source, it is then necessary to precisely identify and study the sources responsible for this nuisance at train pass-by. For speeds up to 300 km/h, rolling noise is the main railway noise source [1]. Among other sources such as the wheels and the sleepers, the rail mainly contributes to rolling noise from approximately 500 Hz to 1000 Hz [2]. Classical array processing methods such as beamforming are commonly used for incoherent source identification in the farfield or point sources in the nearfield, but are not adapted to the rail, due to its extended and coherent nature [3]. Those methods provide least squares or maximum likelihood estimates for one source with white additive noise. Following this principle derived from the estimation theory, a new array processing method is built by resolving a least squares problem adapted to the vibro-acoustical properties of the rail.

In section 2, the acoustic field radiated by the rail is studied for a vertical point excitation, using a Timoshenko beam model for vibrations and a line array of coherent spherical sources for the acoustic radiation. In section 3, an inverse parametric optimisation method is developed in order to estimate unknown parameters of the vibro-acoustical model described in section 2: the amplitudes of N_e uncorrelated excitations (wheel/rail contacts) and the complex wavenumbers that describe the rail vibrations. The performance of the method is investigated, beforehand through simulations in section 4, and then through field testings with a modal shaker in section 5.

2 Acoustic field radiated by a rail

2.1 Rail modelling

When the rail is excited by point forces representing the wheel/rail contacts, vibration waves propagate away from the forcing points. These different waves (vertical and lateral flexural waves, torsion waves, cross-section deformation waves) are characterized by their amplitudes and their complex structural wavenumbers. The resulting displacements of the rail induce acoustic power to be radiated in the free field, with spatial properties depending on the wave properties [4].

For the numerical simulations, only vertical vibrations are considered in this paper, and the rail is represented by a Timoshenko beam which is suitable for frequencies up to 2 kHz [5]. The rail fastening system on a ballasted track is modelled with mass-spring-damper elements (spring-dampers for the rail pads and the ballast and a mass for the sleepers), either periodically or continuously as a stack of spring-damper and mass layers. For a unit vertical point excitation at pulsation ω, located in z_e, in the case of a continuous model, the mobility of the rail is expressed as:

$$\mathcal{V}_\omega(z) = i\omega\left[F_d \mathrm{e}^{-\gamma_d|z-z_e|} + iF_p \mathrm{e}^{-\gamma_p|z-z_e|}\right] \tag{1}$$

where F_d, γ_d, complex, are the amplitude and the wavenumber of a near field wave, and F_p, γ_p are the amplitude and the wavenumber of a potentially propagative wave. Both complex amplitudes F_d and F_p depend on γ_d and γ_p. For a given complex structural wavenumber γ, two quantities are defined from its real and imaginary parts:

- the real wavenumber $k_z = \mathrm{Im}(\gamma)$ representing the propagating part (in m^{-1}),
- the decay rate $\Delta = \mathrm{Re}(\gamma) \cdot 20 \log e$ representing the decaying part (in dB/m).

In practice, the measurement of these two quantities for several waves requires the use of specific methods such as Prony methods [6]. In our case however, in order to validate the model for vertical vibrations up to 2 kHz, such methods are not necessary. The measurement of the global track decay rate with impact hammer has then been used. This quantity which is used as a standard to characterize acoustically a railway track is defined as a limited and discrete integral of the squared displacement along the rail [7]:

$$\Delta_\omega(\mathrm{dB/m}) = \frac{10 \cdot \log \mathrm{e}}{\sum_{z=0}^{z_{max}} \frac{|A_\omega(z)|^2}{|A_\omega(z_e)|^2}\Delta_z} \tag{2}$$

with $A_\omega(z)$ the displacement along the rail at pulsation ω (mobility or accelerance), in response to a point excitation at $z = z_e$.

In figure 1, several decay rates for vertical vibrations are plotted against frequency: the predicted decay rates for the propagative wave and the near-field wave, and the global track decay rate, from predictions and from impact hammer measurements. They relate to the measurement site that will be investigated in section 5. The rail and track parameters that were used for predictions were extracted from previous measurements performed on the same site [8].

The near-field wave is strongly attenuated in the whole frequency range while the behaviour of the propagative wave

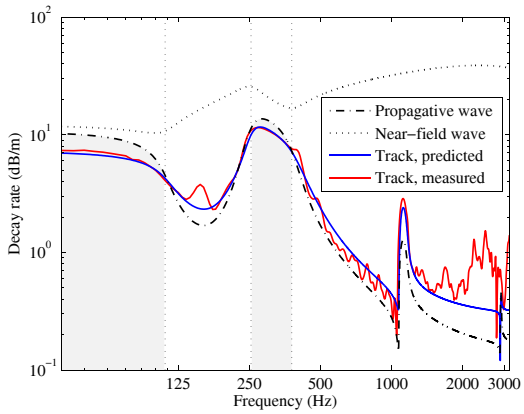

Figure 1: Decay rate of vertical rail vibration, predicted and measured for a periodically supported Timoshenko beam.

is more frequency dependent, with two stop-bands (in grey) in which the wave is strongly attenuated. Those behaviours are related to the resonance frequencies of the spring-damper-mass system. At around 1100 Hz, a peak is observed for the propagative wave and the track decay rates. They are relative to the so-called *pinned-pinned* frequency where the wavelength in the rail is twice the spacing between two sleepers. For the global track decay rate, figure 1 shows good agreement between predictions and measurements up to 2 kHz.

The acoustic equivalent model for the rail is a line array of coherent spherical monopoles with equal spacing along its z-axis [2]:

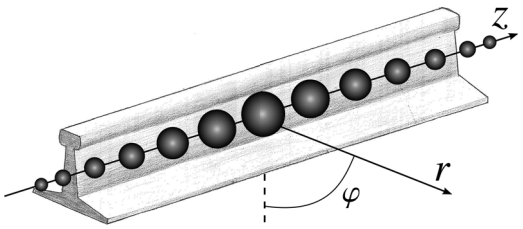

Figure 2: Acoustic equivalent model for the rail.

The amplitude of each monopole located at $z = z_s$ is proportional to the mobility of the rail at the same point. The spatial acoustic field $p(r, z)$ is a superposition of the elementary fields relative to each point source:

$$p(r,z) = i\omega Q_{l_0} \int_{-\infty}^{+\infty} \mathcal{V}_\omega(z_s) \frac{\mathrm{e}^{-ikr_s(z,z_s)}}{4\pi r_s(z,z_s)} \mathrm{d}z_s \qquad (3)$$

where:
(r, z) are the cylindrical coordinates,
$r_s = \sqrt{r^2 + (z - z_s)^2}$ is the distance to the rail axis,
Q_{l_0} is the unit linear mass flow of the rail.

2.2 Spatial characteristics

For the numerical simulations, the integral (3) is limited and sampled, according to convergence tests. For a given frequency, the spacing between two adjacent sources is set to $1/5 \min(\lambda_{\text{air}}, \lambda_{\text{rail}})$ and the z-axis truncation is made when a decay of 60 dB is reached for the rail mobility with regard to the mobility at the nearest excitation. For a single excitation at $z_e = 0$ m, and for a periodically supported model, figure 3 represents the phase of the acoustic field radiated by the rail, for three different frequencies. The corresponding decay rates of the propagative wave are given on top of each map.

For $f = 340$ Hz, vibration waves are strongly attenuated in the rail (17.7 dB/m) and the only part of the rail that radiates acoustic energy in the neighbourhood of the excitation. In this case, the acoustic field has the characteristics of a spherical field as shown in figure 3(a). This particular field could be entirely characterized by the position of a spherical monopole (actually the position of the excitation) and its amplitude. This identification could be performed with a classical beamforming method designed for spherical waves.

For high frequencies, the propagative wave is hardly attenuated (0.28 dB/m here, for $f = 1500$ Hz) and vibration waves propagate over long distances away from the forcing point. In this case, the rail can be acoustically approached by two semi infinite cylindrical monopoles, each being crossed by a monochromatic vibration wave $A\mathrm{e}^{\pm ik_z(z-z_e)}$, where $k_z = \mathrm{Im}(\gamma_p)$. The resulting acoustic field is characterized by an amplitude and a radiation direction θ directly linked to the structural wavenumber as follows [4]:

$$\theta = \arccos\left(k_z/k\right) \qquad (4)$$

where k is the wavenumber in air.

In this case illustrated in figure 3(c), the acoustic field radiated by the rail could be characterized through a classical beamforming designed for plane waves.

For other intermediate cases (*e.g.* for the *pinned-pinned* frequency or for intermediate decay rates), the acoustic field can no more be approached by elementary acoustic sources such as spherical or cylindrical monopoles. Figure 3(b) highlights heterogeneous spatial properties of the field. Additionally, for more complicated cases (multiple wheel/rail contacts for example), this spatial variability will be even greater. There is no immediate beamforming method that could characterize the acoustic field in this case.

The purpose of this study is to design a new array processing method adapted to the specificities of the acoustic field radiated by the rail in the whole frequency range of interest. This new method should include as much knowledge as possible on the source physics *i.e.* location, amplitude and vibro-acoustical characteristics. In section 3, a vibro-acoustical source model is built for the rail. Some of the parameters of this model are then estimated through the minimization of a least square criterion applied to the estimated and modelled spectral matrices on any microphone array.

3 Inverse parametric optimization method adapted to the rail

From section 2, it is obvious that the specificities of the acoustic field radiated by the rail are related to its vibratory behaviour. As long as the rail vibrations can be seen as a superposition of different waves, the resulting acoustic field can then be characterized by these waves properties: amplitudes and wavenumbers. The method proposed here consists in estimating these parameters through an inverse optimisation process.

3.1 Vibro-acoustic source model for the rail

Let us consider N_e uncorrelated complex excitation forces F_n located at $z = z_n$, and a single type of vibration (vertical

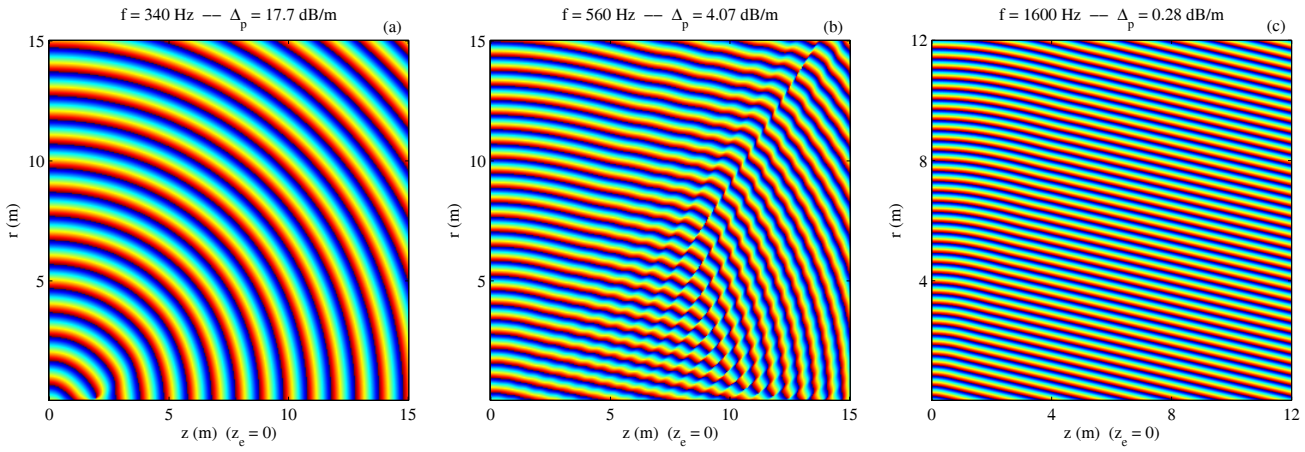

Figure 3: Phase of the acoustic field radiated by a rail for vertical vibrations, with a periodically supported beam model.

bending for example). According to equations (3), the acoustic field in space $p(r,z)$ can be written for a given pulsation as:

$$p(r,z) = \sum_{n=1}^{N_e} \underbrace{i\omega Q_{l_0} F_n}_{A_n} \underbrace{\int_{-\infty}^{+\infty} \mathcal{V}_n\left(z_s; z_n, \underline{\zeta}\right) \frac{\mathrm{e}^{-ikr_s(z,z_s)}}{4\pi r_s(z,z_s)} \mathrm{d}z_s}_{v_n(z_n,\underline{\zeta})} \quad (5)$$

where $\underline{\zeta}$ is the vector containing the unknown wavenumbers for the considered type of vibrations. In the case of vertical bending waves modelled by a Timoshenko beam, according to equation (1), we have: $\underline{\zeta} = {}^t\left[\gamma_d, \gamma_p\right]$.

Finally, the acoustic pressure is evaluated on each microphone of some array to build the vector $\underline{P}$ of dimension N_c equal to the number of microphones:

$$\underline{P} = \sum_{n=1}^{N_e} A_n \underline{v}_n(z_n, \underline{\zeta}) \quad (6)$$

where A_n is the complex vibro-acoustical amplitude of the source n and $\underline{v}_n(z_n,\underline{\zeta})$ is the steering vector associated with the source n (the term *source* refers here to the association of an excitation with a type of wave). In the following, we suppose that the positions z_n are known and we write therefore $\underline{v}_n(\underline{\zeta})$. In practice, the steering vectors $\underline{v}_n(\underline{\zeta})$ are normalized so that $\|\underline{v}_n(\underline{\zeta})\|$ is also included in A_n.

3.2 Least square optimization problem

As the excitation amplitudes are supposed to be random and uncorrelated, they are characterized by their unknown variances $\underline{X} = \left[\sigma_1^2; \ldots; \sigma_{N_e}^2\right]$. Following the probabilistic nature of the problem, the modelled spectral matrix on the array can be written as:

$$\mathbf{\Gamma}^{\mathrm{mod}}\left(\underline{X}, \underline{\zeta}\right) = \sum_{n=1}^{N_e} \sigma_n^2 \, \underline{v}_n(\underline{\zeta}).\underline{v}_n(\underline{\zeta})^\dagger + \sigma_b^2 \mathbf{I} \quad (7)$$

Where $\mathbf{I}$ is the identity matrix and σ_b^2 is the variance of a spatially white gaussian noise. In this paper $\sigma_b^2 = 0$, but the influence of noise on the method is detailed in [8].

The least squares criterion C is the squared error between the modelled and the measured spectral matrices, in terms of the Frobenius norm:

$$C(\underline{X}, \underline{\zeta}) = \sum_{m,n} \left| \widehat{\mathbf{\Gamma}}_{m,n} - \mathbf{\Gamma}^{\mathrm{mod}}_{m,n} \right|^2 = \left\| \widehat{\mathbf{\Gamma}} - \mathbf{\Gamma}^{\mathrm{mod}} \right\|_F^2 \quad (8)$$

where $\widehat{\mathbf{\Gamma}}$ is an estimation of the spectral matrix measured on the array.

The solution of the estimation problem is found by minimizing the criterion C with respect to $\underline{X}$ and $\underline{\zeta}$. Actually, this can be seen as a projection problem. Let $\bar{H}$ be the pre-Hilbert space of the hermitian matrices of size $\mathrm{N_c} \times \mathrm{N_c}$ together with the scalar product $\langle \mathbf{X} | \mathbf{Y} \rangle = \mathrm{tr}\,(\mathbf{X} \cdot \mathbf{Y})$. The set of the $\underline{v}_n(\underline{\zeta})\underline{v}_n^\dagger(\underline{\zeta})$ products provides a subspace of H.

The criterion C reflects the distance between $\widehat{\mathbf{\Gamma}}$ and some matrix $\mathbf{\Gamma}^{\mathrm{mod}}$ in the subspace. For a given $\underline{\zeta}$, this is the minimum distance if and only if $\mathbf{\Gamma}^{\mathrm{mod}}$ is the orthogonal projection of $\widehat{\mathbf{\Gamma}}$ in the subspace generated by the $\underline{v}_n(\underline{\zeta})\underline{v}_n^\dagger(\underline{\zeta})$ matrices. In this linear algebra context, it can be proved that this solution exists and is unique [8]:

$$(\widehat{\underline{X}}, \widehat{\underline{\zeta}}) = \underset{\underline{X},\underline{\zeta}}{\arg\min}\ C \Leftrightarrow \begin{cases} \widehat{\underline{\zeta}} = \underset{\underline{\zeta}}{\arg\max} \underline{U}^t \mathbf{V}^{-1} \underline{U} \\ \widehat{\underline{X}} = \mathbf{V}^{-1} \underline{U}\big|_{\underline{\zeta}=\widehat{\underline{\zeta}}} \end{cases} \quad (9)$$

with, leaving out the $\underline{\zeta}$ dependency for $\underline{v}_n(\underline{\zeta})$,

$\mathbf{V}_{m,n} = \left\langle \underline{v}_m \, \underline{v}_m^\dagger \,|\, \underline{v}_n \, \underline{v}_n^\dagger \right\rangle = \left| \underline{v}_m^\dagger \, \underline{v}_n \right|^2$

$U_n = \underline{v}_n^\dagger \left(\widehat{\Gamma} - \sigma_b^2 \mathbf{I} \right) \underline{v}_n$

From equation (7) there is evidence that the problem is linear with respect to the variances σ_n^2. Thus, an analytical solution is found for $\widehat{X}$ in (9), while the estimation of $\underline{\zeta}$ still requires to minimize a function with $X = \widehat{X}$. In the case of a unique gaussian random source, this solution is equivalent to the solution provided by the maximum likelihood estimator [8, 9]. Moreover, if the steering vectors $\underline{v}$ are designed for a spherical or a plane wave, the solution (9) is equivalent to the one obtained with classical beamforming (where $\underline{\zeta}$ is the source position or direction). This shows that the estimation method proposed here is nothing less than the application of the estimation theory to a more complex problem than those usually treated by beamforming.

3.3 Positivity of the estimated variances

Even if the theory proves the existence and the uniqueness of the solution in any case, it could lead to negative estimations for some σ_n^2 in practice. This renders the fact that the projection basis (the set of $\underline{v}_n \, \underline{v}_n^\dagger$) may not be suitable for the problem. In other terms, this means that we may try to find the characteristics of a source that is not effectively present

or that is not significant. Thus, for a given set of N_e intended sources, when a σ_n^2 is found negative, the problem will be solved for the $2^{N_e} - 1$ cases with at least one of the variances of the sources set to 0. The criterion C is evaluated in each case, and the final solution will be the one that minimizes C.

4 Performance of the method

Beforehand, simulations have been performed to appraise the performance of the method in different cases. This section summarizes the main results. All the measured data have been simulated from a vibro-acoustical model such as presented in section 2.1. The acoustic model is the equivalent line array of spherical monopoles, and the vertical rail vibrations, through $\mathcal{V}_\omega$, are determined from a periodically supported Timoshenko beam model. A line array of 13 equally spaced microphones is used, parallel to the rail axis at 2.5 m from it, with central microphone position z_c varying with respect to the excitations ($z_c \in [z_e; 5\,\text{m}]$ in the case of a single excitation at z_e). For each frequency, the microphone spacing d is set to fulfill the spatial Shannon criterion: $d = \lambda_{\text{air}}/2$.

For the source model and therefore $\mathbf{\Gamma}^{\text{mod}}$, the same equivalent acoustic model is used (Fig. 2) while different models for the rail vibrations are tested, more or less simplified. For a given problem, $\underline{X}$ and $\underline{\zeta}$ are estimated from equation (9) and the acoustic field is rebuilt from equation (3). The representativeness of the rebuilt (estimated) acoustic field compared with the true (simulated) field is then evaluated in terms of the following criterions:

- Total acoustic power radiated by the rail.
- Average directivity of the acoustic field along a line parallel to the rail (at 2.5 m and 7.5 m).
- Average squared acoustic pressure along the same line.

In a first step, the source model is built assuming the $\underline{\zeta}$ parameters (*i.e.* the complex wavenumbers) to be known. In this case, the optimization process only concerns the estimation of the variances $\underline{\widehat{X}}$ which is analytically performed according to (9). It has been shown that:

- Additive noise has only a slight influence on $\underline{\widehat{X}}$ (less than 0.7 dB error for 0 dB SNR).
- The method is robust with respect to errors on the wavenumbers as long as the array centre is in front of the excitation.
- A simplified continuously supported Euler beam source model ($\gamma_d = -i\gamma_p$ and $F_d = F_p$) can be used for vibrations, except for the *pinned-pinned* frequency.

In a second step, the parameters $\underline{\zeta}$ are estimated simultaneously with the variances $\underline{X}$. In order to evaluate the method independently of any numerical optimization algorithm, the simplified 'continuous-Euler' model is assumed for the source model, which means that only one complex wavenumber is unknown: $\underline{\zeta} = {}^t[\Delta, k_z]$. The fonction $F = \underline{U}^t\mathbf{V}^{-1}\underline{U}$ to be minimized can then be plotted and studied in a 2-Dimensional (Δ, k_z) discrete and bounded space, allowing reliable values for Δ and k_z and sufficient precision. It has been shown that:

- For high decay rates, the shape of F is quite flat and the discriminatory ability of the method is limited, both for Δ and k_z estimation. For lower decay rates the method is very selective regarding k_z, and only slightly better for Δ.
- The resolution is better when the array is away from the excitations.
- The simplified 'continuous-Euler' source model leads to good estimates of γ_p (wavenumber of the propagative wave of the true 'Periodical-Timoshenko' model), even at the *pinned-pinned* frequency.

Figure 4 is an example plot for F, in the case of a 'periodical-Timoshenko' true model *versus* 'continuous-Euler' source model. The estimated wavenumber (+) is very close to the wavenumber of the propagative wave for the true model (∘). It was found that the reconstructed acoustic field is representative of the true field except for the directivity at the *pinned-pinned* frequency, since the track was supposed to be continuous in the source model.

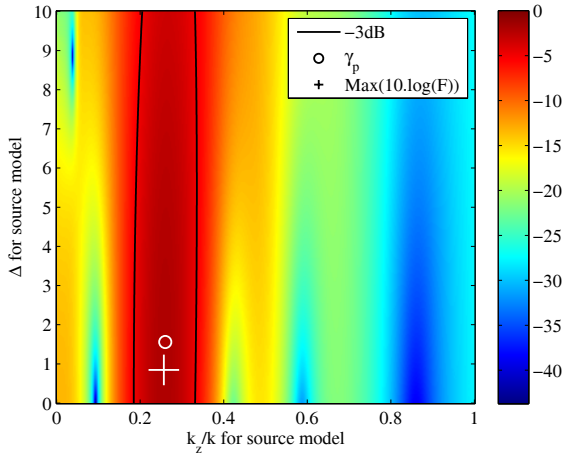

Figure 4: 2-dimensional plot of $10\log F$ for a simplified 'continuous-Euler' source model at *pinned-pinned* frequency. Excitation between two sleepers, $z_c = 3$ m.

From this numerical study, some inner parameters of the method can now be fixed to provide the best performances for reduced complexity. First, the source model can be based on a simplified 'Continuous-Euler' model. The variance of the sources should be estimated when the array is close to them and the other parameters (the complex wavenumbers) should be estimated when the array is shifted away from the sources (about 3 m).

5 Acoustic measurements

A 30 m long rail is periodically supported on a classical ballasted track, with resilient boots under the sleepers accounting for the ballast. The rail is vertically excited by a modal shaker between two sleepers (ref. $z_e = 0$ m) near the middle of the rail length. A linear array of 21 microphones is parallel to the rail axis, at $R = 2.64$ m from this latter, with centre microphone abscissa $z_c = 3$ m. The array is made of two nested sub-arrays of 13 microphones with different apertures, which are used as follows: the array with the microphone spacing $d = 15$ cm is used for frequencies up to 2000 Hz and the one with $d = 5$ cm is used beyond. The experimental set-up is shown in figure 5.

Figure 5: Experimental set-up.

The excitation is a pseudo-random signal (amplitude modulation) centred around the centre frequency of each third-octave band from 160 Hz to 3150 Hz. The method described in section 3 is applied to find the complex wavenumber $\underline{\zeta} = {}^t[\Delta, k_z]$ of a 'continuous-Euler' source model, such as in section 4. Figure 6 represents the wavenumber (a) and the decay rate (b) of the propagative vertical bending wave, estimated with our method applied to the measurements, and predicted from a fitted 'periodic-Timoshenko' model (see Fig. 1).

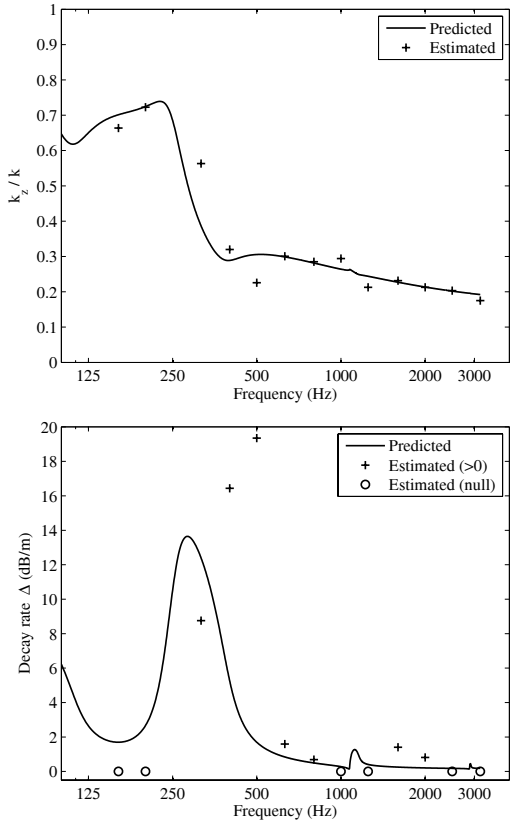

Figure 6: Wavenumber (a) and decay rate (b) of the vertical bending wave in the rail (γ_p), estimated and predicted.

The wavenumbers are well estimated, especially for frequencies that correspond to low decay rates, where the acoustic field radiated by the rail becomes cylindrical. When the decay rate is high, as predicted by the simulations, the method is less discriminant: at 316 Hz k_z is estimated with some error, at 250 Hz the method did not even provide a solution (no convergence in the plan considered). The decay rates are also better estimated for low values, but some of them were found null. In those cases as well as for strongly overestimated high decay rates, simulations proved that the acoustic field remains correctly rebuilt [8].

6 Conclusion

In this paper, the acoustic field radiated by the rail is characterized with a linear microphone array, through an inverse parametric optimisation method. The method is based on the least square criterion applied to the measured and the modelled spectral matrices on the array. The vibro-acoustical model chosen for the rail is a superposition of structural waves for the vibration and a line array of spherical acoustic monopoles for the radiation. The estimated parameters are the wavenumbers and the amplitudes of the N_e uncorrelated sources of the model (*i.e.* N_e associations of an excitation with a type of wave). In a first step, simulations have been performed to appraise the efficiency of the method. The estimation of the amplitudes is robust with respect to modelling errors when the excitations are in front of the array centre. For the estimation of the wavenumbers, the method is more discriminant when the array is away from the forcing point. Finally, the proposed method has been validated *in situ* for the vertical bending of a rail excited with a modal shaker: the results are correct, except at frequencies for which the waves are strongly attenuated.

References

[1] C. Mellet, F. Létourneaux, F. Poisson, C. Talotte, "High speed train noise emission: Latest investigation of the aerodynamic/rolling noise contribution", *Journal of Sound and Vibration* **293**(3-5), 535-546 (2006)

[2] D.J. Thompson, C.J.C. Jones, "A review of the modelling of wheel/rail noise generation", *Journal of Sound and Vibration* **231**(3), 519-536 (2000)

[3] T. Kitagawa, D.J. Thompson, "The horizontal directivity of noise radiated by a rail and implications for the use of microphone arrays", *Journal of Sound and Vibration* **329**(2), 202-220 (2010)

[4] D.J. Thompson, C.J.C. Jones, N. Turner, "Investigation into the validity of two-dimensional models for sound radiation from waves in rails", *J. Acoust. Soc. Am.* **113**(4), 1965-1974 (2003)

[5] K. Knothe, S. Grassie, "Modelling of Railway Track and Vehicle/Track Interaction at High Frequencies", *Vehicle System Dynamics: International Journal of Vehicle Mechanics and Mobility* **22**(3), 209-262 (1993)

[6] K. Grosh, E.G. Williams, "Complex wave-number decomposition of structural vibration", *J. Acoust. Soc. Am.* **93**(2), 836-848 (1993)

[7] CEN, European Committee for Standardization, "Railway applications - Noise emission - Characterisation of the dynamic properties of track sections for pass by noise measurements", EN 15461, (2008)

[8] B. Faure, "Caractérisation du rayonnement acoustique d'un rail à l'aide d'un réseau de microphones", *Université de Grenoble*, PhD thesis (2011)

[9] S. Marcos "Méthodes à haute résolution : traitement d'antenne et analyse spectrale", *Collection Traitement du Signal*, HERMES (1998)